Linear σ Model and the Observed Enhancement in the Mass Spectrum of $p\bar{p}$ in $J/\psi \to \gamma p\bar{p}$ *

LIU Xiang[1] ZENG Xiao-Qiang[1] DING Yi-Bing[3] LI Xue-Qian[1,2;1)]
SHEN Hong[1] SHEN Peng-Nian[2,4]

1 (Department of Physics, Nankai University, Tianjin 300071, China)
2 (Institute of Theoretical Physics, CAS, Beijing 100080, China)
3 (Department of Physics, Graduate University of the Chinese Academy of Sciences, Beijing 100049, China)
4 (Institute of High Energy Physics, CAS, Beijing 100049, China)

Abstract Provided the enhancement in the $p\bar{p}$ spectrum in radiative decay $J/\psi \to \gamma p\bar{p}$ observed by the BES collaboration is due to an existence of a $p\bar{p}$ molecular state, we calculate its binding energy and lifetime in the linear σ model. Concretely, we consider a possibility that the enhancement is due to a $p\bar{p}$ resonance which is in either S-wave or P-wave structure and compare our results with the data. Moreover, $p\bar{p}$ can annihilate at s-channel which is absent in deuteron, thus by studying the total width of the $p\bar{p}$ bound state, we may gain more information about the linear σ model and some concerned issues.

Key words linear σ-model, J/ψ decay, resonance, annihilation

1 Introduction

Existence of σ particle is still in dispute. If it indeed exists as a physical particle of 0^{++}, the linear σ model would be an appropriate model for dealing with the interaction between hadrons. There have been flood of works to discuss the applicability of the linear σ model. In any practical calculations the expansion in momentum must be truncated, namely higher orders are dropped out. On the other hand, several phenomenological models, such as the Paris potential, can result in numbers which are consistent with data, not only for the mass spectra of hadrons, but also the phase shifts of the hadron scattering at lower energies. One cannot, definitely, expect that the results obtained in the non-linear σ model can be as precise as that gained in, say, the Paris potential, however, one can achieve information about the long expecting σ boson. This information is valuable to both theorists and experimentalists of nuclear and particle physics.

Recently, the BES Collaboration has observed a near-threshold enhancement in the $p\bar{p}$ mass spectrum in the radiative decay $J/\psi \to \gamma p\bar{p}$[1]. Later similar enhancement has been reported by the Belle Collaboration in $\bar{B}^0 \to D^{(*)0} p\bar{p}$ and $B^{\pm} \to p\bar{p}K^{\pm}$ decays [2, 3].

A plausible interpretation is that there exists a $p\bar{p}$ bound state of either 0^{-+} or 0^{++}, and if it is the case, the BES data favor the value of

$$m = 1859^{+3}_{-10}(\text{stat})^{+5}_{-25}(\text{syst})\,\text{MeV} \quad \text{and} \quad \Gamma < 30\,\text{MeV}.$$

There have also been various interpretations for the observed enhancement. The enhancement can be understood if the final state interaction between p and $\bar{p}$ is properly considered, as some authors suggested[4]. Meanwhile in analog to $a_0(980)$ and $f_0(980)$ which are supposed to be molecular states of $K\bar{K}$, it is tempted to assume that $p\bar{p}$ constitute a bound state with

Received 20 June 2005, Revised 9 August 2005
*Supported by National Natural Science Foundation of China (10475202, 10475089, 10435080), Research Fund for the Doctoral Program of Higher Education of China, Knowledge Innovation Key Project of CAS (KJCX2-SW-N02) and IHEP (U529)
1) E-mail: lixq@nankai.edu.cn

quantum number 0^{-+} or 0^{++}.

To get an insight in the structure, one needs to evaluate the corresponding binding energy and lifetime, then compare the theoretical results with the data. In this work, we employ the linear σ model. Historically, there has been dispute about the linear σ model where the σ meson stands as a realistic scalar meson[5] whereas in alternative scenarios, it is suggested that the contribution of σ can be attributed to two-pion exchange[6]. In fact, the difference between the linear σ model and non-linear σ model is whether the 0^{++} σ meson is a substantial object, it corresponds to the linear or non-linear realization of the chiral lagrangian[7]. Because the low-energy QCD which is the underlying theory of hadron physics, is fully non-perturbative, all the coefficients in the effective Lagrangian are so far not derivable, but must be obtained by fitting data. Therefore determination of the coefficients is somehow model-dependent and phenomenological. It is believed that at least for the leading order, all models would be applicable, even though they look somewhat different. As we employ the linear σ model which is simpler in calculations, we take all the coefficients by fitting data.

In our earlier work[8], we used the linear σ model to calculate the properties of deuteron, and by fitting data we not only determine the value of m_σ but also fix the corresponding parameters of the linear σ model. In this work we will use the same model with the parameters obtained by fitting the deuteron data to carry out calculations for the $\mathrm{p\bar{p}}$ bound state. On the other side, deuteron consists of proton and neutron, thus there is no s-channel annihilation, whereas for $\mathrm{p\bar{p}}$ bound state, the channel is open, so that more contributions and complications would come up. By studying the system, we would gain more knowledge on the linear σ model and the parameters. The nucleon-antinucleon interaction and the effective potential were studied almost half centuries ago in phenomenological approach[9, 10]. Our approach is based on the linear σ model which attracts much attention recently and may play an important role for understanding the meson family.

The present BES data do not finally decide if the resonance is an S-wave or P-wave bound state, but only indicate that the position of the S-wave peak is below the threshold $2m_{\mathrm{p}}$ whereas the peak of the P-wave is a bit above the threshold. In our model, since the effective potential for the S-wave is attractive except a repulsive core near $r \to 0$, the binding energy must be negative, so that the calculated mass of the S-wave bound state is below the $2m_{\mathrm{p}}$ threshold. Whereas for the P-wave due to the angular momentum barrier which is non-zero and positive, the binding energy becomes positive and the total mass is greater than $2m_{\mathrm{p}}$. This interpretation is consistent with the observation of BES.

To evaluate the total width of the bound state, we need to achieve the imaginary part of the potential which is induced by the absorptive part of the loops in the $\mathrm{p\bar{p}}$ elastic scattering amplitude (see the text for the concerned Feynman diagrams and some details). Thus according to the traditional method[11], we derive the real part of the potential which mainly comes from the tree-level scattering amplitude where t-channel mesons are exchanged, including σ, π, ρ and ω. For the S-wave bound state not only t-channel exchange, but also the s-channel annihilation contribute. Namely in the s-channel, η, η′, η(1295) and η(1440) are the intermediate mesons and they contribute both real and an imaginary parts to the effective potential. Moreover, there exist box diagrams, whose absorptive part contributes an imaginary effective potential to either S-state or P-state. Thus the eigenenergy becomes $E_{\mathrm{Re}} - \mathrm{i}\dfrac{\Gamma}{2}$ and the time-factor is $\exp(-\mathrm{i}E_{\mathrm{Re}}t - \dfrac{\Gamma}{2}t)$ and the Γ corresponds to the total width and $E_{\mathrm{Re}} - \mathrm{i}\dfrac{\Gamma}{2}$ is a solution of the Schrödinger equation with a complex potential.

For the P-wave, besides the mechanism discussed above, since the binding energy is positive, the bound state may dissolve into $\mathrm{p} + \bar{\mathrm{p}}$ final state via quantum tunnelling. By the WKB approximation method[12], the tunnelling transition probability is $\exp[-2\int_a^b \sqrt{2\mu(V-E)}\mathrm{d}r]$, thus the total width of the P-wave bound state would be $2\mu \exp[-2\int_a^b \sqrt{2\mu(V-E)}\mathrm{d}r]$, where $\mu = \dfrac{m_{\mathrm{p}}}{2}$ is the

reduced mass. Our numerical results show that the dissociation rate via tunnelling is much smaller than the decays because of the phase space of the final state.

Substituting the potential no matter real and complex, into the Schrödinger equation, and solving it, one obtains both the eigenenergies and eigenfunctions of both S-wave and P-wave bound states. Then we can evaluate the masses and total widths of the bound states. That is the strategy of this work. In this work, however, we adopt a simple way, namely to avoid the complexity and get insight in the picture, we only substitute the real part of the potential into the Schrödinger equation and use the perturbation method to evaluate the contribution from the s-channel annihilation (for S-wave only) and that from box diagrams (for both S- and P-waves), as well as the total width.

This paper is organized as follows. After this introduction, we derive the formulation for the complex potential with a brief introduction of the linear σ model. In Sec. Ⅲ, we substitute the potential into the Schrödinger equation and solve it to obtain the numerical result of the eigenenergy and eigenfunction, then obtain the masses and widths of the S- and P-wave bound states. In the section we also present all relevant parameters. The last section is devoted to our conclusion and discussion. Some complicated and lengthy expressions are collected in the appendix.

2 The formulation

2.1 The necessary information about the model

In the linear σ model, the effective Lagrangian is

$$L = g\bar{\psi}(\sigma + \mathrm{i}\gamma_5 \boldsymbol{\tau}\cdot\boldsymbol{\pi})\psi, \tag{1}$$

where ψ is the wavefunction of the nucleon. When we calculate the scattering amplitude, we introduce a form factor to compensate the off-shell effects of the exchanged mesons. For the t-channel exchange, at each vertex, the form factor is written as[8]

$$\frac{\Lambda^2 - M_{\mathrm{m}}^2}{\Lambda^2 - q^2}, \tag{2}$$

where Λ is a phenomenological parameter and its value is near 1 GeV. It is observed that as $q^2 \to 0$ it becomes a constant and if $\Lambda \gg M_{\mathrm{m}}$, it turns to be unity. In the case, as the distance is infinitely large, the vertex looks like a perfect point, so the form factor is simply 1 or a constant. Whereas, as $q^2 \to \infty$, the form factor approaches to zero, namely, in this situation, the distance becomes very small, the inner structure (quark, gluon degrees of freedom) would manifest itself and the whole picture of hadron interaction is no longer valid, so the form factor is zero which cuts off the end effects. Indeed, there are many other form factors to describe the physics picture.

To derive an effective potential, one sets $q_0 = 0$ and writes down the elastic scattering amplitude in the momentum space and then carries out a Fourier transformation turning the amplitude into an effective potential in the configuration space. Following the standard procedure[11], we derive the effective potential from the scattering amplitude. Below, we present some details about the individual parts of the potential.

2.2 The effective potentials

2.2.1 The real part of the potential

Here we first consider the meson exchanges at the t-channel, because the intermediate meson is space-like, it cannot be on its mass-shell, so that does not contribute to the imaginary part of the effective potential. Then we will go on discussing the s-channel contributions.

(a) Via exchanging π-meson:

The effective vertex is

$$L = \mathrm{i}g\bar{\psi}\gamma_5 \boldsymbol{\tau}\cdot\boldsymbol{\pi}\psi, \tag{3}$$

and obviously only π^0 can be exchanged in our case.

The scattering amplitude in the momentum space is

$$V_\pi(\boldsymbol{q}) = \frac{g_{\mathrm{NN}\pi}^2}{4m_{\mathrm{p}}^2(\boldsymbol{q}^2 + m_\pi^2)}(\boldsymbol{\sigma}_1\cdot\boldsymbol{q})(\boldsymbol{\sigma}_2\cdot\boldsymbol{q})\left(\frac{\Lambda^2 - m_\pi^2}{\Lambda^2 + \boldsymbol{q}^2}\right)^2. \tag{4}$$

Following the standard procedure, we carry out a Fourier transformation on $V_\pi(\boldsymbol{q})$ and obtain the effec-

tive potential in the configuration space:

$$V_\pi(r)=-\frac{g^2_{\rm NN\pi}}{4m^2_{\rm p}}(\boldsymbol{\sigma}_1\cdot\boldsymbol{\nabla})(\boldsymbol{\sigma}_2\cdot\boldsymbol{\nabla})f_\pi(r)\ , \tag{5}$$

where

$$f_\pi(r)=\frac{{\rm e}^{-m_\pi r}}{4\pi r}-\frac{{\rm e}^{-\Lambda r}}{4\pi r}+\frac{(m^2_\pi-\Lambda^2){\rm e}^{-\Lambda r}}{8\pi\Lambda}. \tag{6}$$

(b) Via σ and ρ and ω exchanges.

The effective vertices are respectively

$$L_\sigma=g\bar\psi\psi\sigma, \tag{7}$$

$$L_\rho=g_{\rm NN\rho}\bar\psi\gamma_\mu\tau^a\psi A^{a\mu},\quad a=1,2,3, \tag{8}$$

$$L_\omega=g_{\rm NN\omega}\bar\psi\gamma_\mu\psi\omega^\mu. \tag{9}$$

The scattering amplitude via exchanging σ-meson is

$$\begin{aligned}V_\sigma(\boldsymbol{q})\ =\ &-\frac{g^2_{\rm NN\sigma}}{4m^2_{\rm p}(\boldsymbol{q}^2+m^2_\sigma)}\big[4m^2_{\rm p}-4\boldsymbol{p}^2-\boldsymbol{q}^2-\\&4(\boldsymbol{p}\cdot\boldsymbol{q})-{\rm i}\,\boldsymbol{\sigma}\cdot(\boldsymbol{q}\times\boldsymbol{p})\big]\left(\frac{\Lambda^2-m^2_\sigma}{\Lambda^2+\boldsymbol{q}^2}\right)^2,\end{aligned}$$

through a Fourier transformation, the potential is

$$\begin{aligned}V_\sigma(r)\ =\ &-\frac{g^2_{\rm NN\sigma}}{4m^2_{\rm p}}\Big[4m^2_{\rm p}f_\sigma(r)-4\boldsymbol{p}^2f_\sigma(r)+\boldsymbol{\nabla}^2f_\sigma(r)+\\&4{\rm i}(\boldsymbol{p}\cdot\boldsymbol{r})F_\sigma(r)-2(\boldsymbol{L}\cdot\boldsymbol{S})F_\sigma(r)\Big],\end{aligned}$$

where

$$\begin{aligned}f_\sigma(r)\ &=\ \frac{{\rm e}^{-m_\sigma r}}{4\pi r}-\frac{e^{-\Lambda r}}{4\pi r}+\frac{(m^2_\sigma-\Lambda^2){\rm e}^{-\Lambda r}}{8\pi\Lambda}\\F_\sigma(r)\ &=\ \frac{1}{r}\frac{\partial}{\partial r}f_\sigma(r).\end{aligned}$$

Via exchanging vector-meson ρ (only ρ^0 contributes), the effective potential is

$$\begin{aligned}V_\rho(r)\ =\ &\frac{g^2_{\rm NN\rho}}{4m^2_{\rm p}}\Big[4m^2_{\rm p}f_\rho(r)-\boldsymbol{\nabla}^2f_\rho(r)+\\&4\boldsymbol{p}^2f_\rho(r)+2(\boldsymbol{L}\cdot\boldsymbol{S})F_\rho(r)-4{\rm i}(\boldsymbol{p}\cdot\boldsymbol{r})F_\rho(r)+\\&(\boldsymbol{\sigma}_1\cdot\boldsymbol{\nabla})(\boldsymbol{\sigma}_2\cdot\boldsymbol{\nabla})f_\rho(r)\Big]\end{aligned}$$

where

$$\begin{aligned}f_\rho(r)\ &=\ \frac{{\rm e}^{-m_\rho r}}{4\pi r}-\frac{{\rm e}^{-\Lambda r}}{4\pi r}+\frac{(m^2_\rho-\Lambda^2){\rm e}^{-\Lambda r}}{8\pi\Lambda}\\F_\rho(r)\ &=\ \frac{1}{r}\frac{\partial}{\partial r}f_\rho(r).\end{aligned}$$

For exchanging an ω vector meson, the expression is similar to that in the ρ case, but has an opposite sign to the ρ contribution due to the G-parity[13, 14], thus one only needs to replace the corresponding parameter values, such as the mass and coupling constant for ρ by that for ω and add a minus sign in front of all the terms of $V_\rho(r)$. For saving space, we dismiss the concrete expression for ω exchange. The details about the potential are collected in the appendix.

(c) The real part of the potential

A synthesis of all the individual contributions derived above stands as the real part of the effective potential, namely the traditional part of the effective potential as

$$\begin{aligned}V_{\rm eff}(r)\ =\ &V_\pi(r)+V_\sigma(r)+V_\rho(r)+V_\omega(r)=\\&V_0(r)+V_{(\boldsymbol{L}\cdot\boldsymbol{S})}(r)+V_{\rm pet}(r)+V_{\rm tensor}+V_{(\boldsymbol{\sigma}_1\cdot\boldsymbol{\sigma}_2)}.\end{aligned}$$

(d) The case of $p\bar p$ is different from the deuteron where the constituents are p and n, namely there is a $p\bar p$ annihilation at the s-channel, which would contribute a delta function to the real part of the effective potential.

If $p\bar p$ is in S-wave, its quantum number is $0^+(0^{-+})$, at the s-channel only a $0^+(0^{-+})$ meson can propagate, here we only consider the lowest-lying pseudoscalar mesons of 0^{-+}, η, η′, η(1295) and η(1440), their contributions are

$$\begin{aligned}V_{\rm anni}(r)\ =\ &\frac{g^2_{\rm NN\eta(\eta')}}{(4m^2_{\rm p}-m^2_{\eta(\eta')})}f(P^2)^2\times\\&\left[-1+\frac{(\boldsymbol{\sigma}_1\cdot\boldsymbol{\nabla})(\boldsymbol{\sigma}_2\cdot\boldsymbol{\nabla})}{2m^2_{\rm p}}-\frac{\boldsymbol{\nabla}^2}{2m^2_{\rm p}}\right]\delta^3(\boldsymbol{r}),\end{aligned}$$

where m is the invariant mass $\sqrt{(p_1+p_2)^2}$ and p_1, p_2 are the four-momenta of the constituents p and $\bar{\rm p}$ respectively. The form factor $f(P^2)$ is different from that obtained before, because this is an s-channel annihilation process and in general, is more suppressed. We will present its concrete form in next subsection. Due to the annihilation suppression, the contribution from the annihilation process to the real part of the effective potential is much smaller than that from the t-channel meson-exchange, so that we can deal with is as a perturbation when we calculate the mass spectrum.

2.2.2 The imaginary part of the complex potential

The corresponding Feynman diagrams are shown in Figs. 1 and 2. Fig. 1 is the self-energy of the intermediate mesons which are off-shell and Fig. 2 is a box diagram. Obviously, the s-channel annihilation

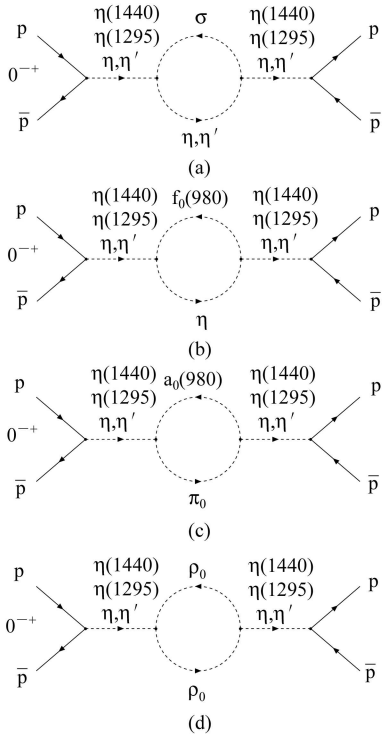

Fig. 1.

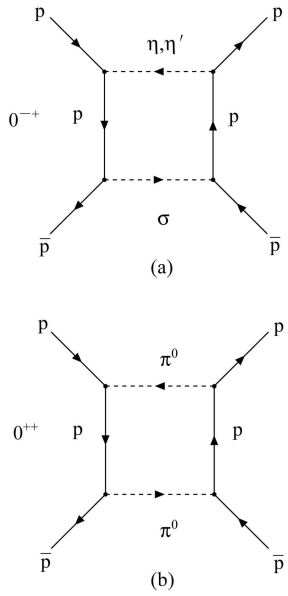

Fig. 2.

of pp̄ is a strong-interaction process, so that parity, isospin, and other quantum numbers must be conserved and as long as the pp̄ bound state is of the 0^{-+} structure, only a few measons (η, η′ η(1295) and η(1440)) can be mediated in the s-channel. Due to the pole structure of the propagator $1/(P^2 - M_{\rm M}^2)$ where $M_{\rm M}$ is the mass of the s-channel intermediate meson and $P^2 = m^2 \approx 4m_{\rm p}^2$ is the mass of the observed bound state, only the mesons whose masses are to m make substantial contributions. In our case as $m \sim 1859$MeV, the main contributions come from $\eta(1295)$ and $\eta(1440)$.

(a) The form factor for the s-channel annihilation is different from that obtained before because the special annihilation suppression. Therefore we adopt another ansatz as

$$\exp\Big[-\frac{\alpha^2}{|P^2 - M_{\rm M}^2|}\Big], \tag{10}$$

where $P = p_1 + p_2$. The parameter α would be fixed by fitting data of BES[1].

(b) The concerned couplings are[15—17]

$$L_{\rm PP\sigma} = -\frac{\gamma_{\rm PP\sigma}}{\sqrt{2}}\,\sigma\,\partial_\mu \boldsymbol{P}\cdot\partial_\mu \boldsymbol{P}, \tag{11}$$

$$L_{\rm VVP} = g_{\rm VVP}\varepsilon^{\mu\nu\lambda\sigma}\,\partial_\mu V_\nu(\boldsymbol{P}\cdot\partial_\lambda \boldsymbol{V}_\sigma), \tag{12}$$

here $\boldsymbol{P}$ stands as pseudoscalar mesons, and $\boldsymbol{V}$ denotes vector mesons.

The imaginary part of the potential is obtained in the following way. First, we calculate the absorptive part of the loops by the Cutkosky cutting rule in the momentum space[18] and carry out a Fourier transformation turning it into an imaginary part of the complex potential.

(c) The contribution induced by the self-energy of 0^{-+} mesons. The corresponding Feynman diagrams are shown in Fig. 1 (a) to (d).

We obtain

$$V_{\rm Im_1}(r) = -\frac{\gamma^2_{\rm M\sigma\eta(\eta')} g^2_{\rm NNM}(4m_{\rm p}^2 - m_\sigma^2 + m^2_{\eta(\eta')})^2}{512\pi m_{\rm p}^2(4m_{\rm p}^2 - M_{\rm M}^2)^2}\times \sqrt{-16m_{\rm p}^2 m^2_{\eta(\eta')} + (4m_{\rm p}^2 - m_\sigma^2 + m^2_{\eta(\eta')})^2}\times f(P^2)^2\delta^3(\boldsymbol{r}),$$

for Fig. 1(a),

$$V_{\rm Im_2}(r) = -\frac{\gamma^2_{\rm M\eta f_0} g^2_{\rm NNM}(4m_{\rm p}^2 - m_{\rm f_0}^2 + m_\eta^2)^2}{512\pi m_{\rm p}^2(4m_{\rm p}^2 - M_{\rm M}^2)^2}\times \sqrt{-16m_{\rm p}^2 m_\eta^2 + (4m_{\rm p}^2 - m_{\rm f_0}^2 + m_\eta^2)^2}\times f(P^2)^2\delta^3(\boldsymbol{r}),$$

for Fig. 1(b),

$$V_{\mathrm{Im}_3}(r) = -\frac{\gamma^2_{\pi\mathrm{Ma}_0} g^2_{\mathrm{NNM}} (4m_{\mathrm{p}}^2 - m_{\mathrm{a}_0}^2 + m_\pi^2)^2}{512\pi m_{\mathrm{p}}^2 (4m_{\mathrm{p}}^2 - M_{\mathrm{M}}^2)^2} \times \sqrt{-16m_{\mathrm{p}}^2 m_\pi^2 + (4m_{\mathrm{p}}^2 - m_{\mathrm{a}_0}^2 + m_\pi^2)^2} \times f(P^2)^2 \delta^3(\boldsymbol{r}),$$

for Fig. 1(c), and

$$V_{\mathrm{Im}_4}(r) = -\frac{g^2_{\mathrm{M}\rho\rho} g^2_{\mathrm{NNM}} (16m_{\mathrm{p}}^4 - 4m_{\mathrm{p}}^2 m_\rho^2)}{128\pi m_{\mathrm{p}}^2 (4m_{\mathrm{p}}^2 - M_{\mathrm{M}}^2)^2} \times \sqrt{16m_{\mathrm{p}}^4 - 16m_{\mathrm{p}}^2 m_\rho^2} f(P^2)^2 \delta^3(\boldsymbol{r}),$$

for Fig. 1(d).

As discussed above, due to the pole structure only $\eta(1295)$ and $\eta(1440)$ which have the right quantum numbers make substantial contributions. Therefore in the equations, the mass M_{M} only take 1293MeV and 1440MeV (taking an average)[19].

Obviously, this s-channel annihilation process only contributes an imaginary part to the bound state of $\mathrm{p\bar{p}}$ where p and $\bar{\mathrm{p}}$ reside in an S-state.

(d) The contributions induced by the box diagram

The diagrams are shown in Fig. 2 and they can contribute an imaginary part to the potential of either S-state or P-state. In these diagrams, we ignore the contributions from vector mesons in the box, this can be taken as an approximation which does not influence the qualitative conclusion. In the last section we will discuss this issue in detail. In fact, Dover and Richard discussed the possible contribution of such box diagrams to the inelastic $\mathrm{p\bar{p}}$ cross section in the optical model[20].

It is noted that even though we calculate the absorptive part of the box, it is not a pure $\mathrm{p\bar{p}}$ scattering process, because they are bound in a 0^{-+} (S-wave) or 0^{++} (P-wave) state. Therefore, by a simple analysis on the total isospin, parity, charge conjugation and angular momentum, the only pseudoscalar mesons in the box must be $\eta(\eta')\sigma$ for 0^{-+} and $\pi\pi$ for 0^{++}.

The absorptive part of the box diagram with $\eta(\eta')\sigma$ as the intermediate pseudoscalars is formulated as (Fig. 2(a))

$$\begin{aligned} V_{\mathrm{Im}_{\mathrm{box}(0^{-+})}}(\boldsymbol{q}) =& 2g^2_{\mathrm{NN}\sigma} g^2_{\mathrm{NN}\eta(\eta')} \int \frac{\mathrm{d}^4 l}{(2\pi)^4} \overline{v}(p_2) \times \\ & \frac{\not{p}_1 - \not{l} + m_{\mathrm{p}}}{(p_1 - l)^2 - m_{\mathrm{p}}^2} \gamma^5 u(p_1) \overline{u}(p_3) \gamma^5 \times \\ & \frac{\not{p}_3 - \not{l} + m_{\mathrm{p}}}{(p_3 - l)^2 - m_{\mathrm{p}}^2} v(p_4) (\mathrm{i}\pi)^2 \times \\ & \delta(l^2 - m^2_{\eta(\eta')}) \delta((p_1 + p_2 - l)^2 - m_\sigma^2) \times \\ & \Big(\frac{\Lambda^2 - m_{\mathrm{p}}^2}{(p_1 - l)^2 - \Lambda^2}\Big)^2 \Big(\frac{\Lambda^2 - m_{\mathrm{p}}^2}{(p_3 - l)^2 - \Lambda^2}\Big)^2, \end{aligned} \tag{13}$$

where

$$\begin{aligned} p_1 + q &= p_3, \\ p_4 + q &= p_2, \\ \boldsymbol{p}_2 &= -\boldsymbol{p}_1. \end{aligned}$$

Eq. (13) is obviously Lorentz invariant, but to carry out this integration, some approximations are necessary. For getting an effective potential, we need making a Fourier transformation later, therefore according to the standard procedure we set $q_0 = 0$, then we have

$$\begin{aligned} V_{\mathrm{Im}_{\mathrm{box}(0^{-+})}}(\boldsymbol{q}) =& -\frac{1}{16\pi^2} \int_0^{2\pi} \mathrm{d}\varphi \int_0^{\pi} \mathrm{d}\theta \sin\theta [-m_{\mathrm{p}}^2 + 2m_{\mathrm{p}}(p_1^0 - l^0) - (p_1^0 - l^0)^2] \frac{1}{8p_1^0} \times \\ & \frac{(\Lambda^2 - m_{\mathrm{p}}^2)^4}{\mathscr{A}(\mathscr{A} + 2|\boldsymbol{l}||\boldsymbol{q}|\cos\alpha)(\mathscr{A} - \Lambda^2 + m_{\mathrm{p}}^2)^2 (\mathscr{A} - \Lambda^2 + m_{\mathrm{p}}^2 + 2|\boldsymbol{l}||\boldsymbol{q}|\cos\alpha)^2}, \end{aligned} \tag{14}$$

here

$$\begin{aligned} \mathscr{A} &= -2p_1^0 l^0 + 2|\boldsymbol{p}_1||\boldsymbol{l}|\cos\theta + l^{0\,2} - \boldsymbol{l}^2, \qquad l^0 = \sqrt{m^2_{\eta(\eta')} + \boldsymbol{l}^2}, \\ |\boldsymbol{l}| &= \frac{1}{4p_1^0} \sqrt{16m_{\mathrm{p}}^4 + 8(m^2_{\eta(\eta')} - m_\sigma^2)m_{\mathrm{p}}^2 + m^4_{\eta(\eta')} + m_\sigma^4 - 2m^2_{\eta(\eta')}(m_\sigma^2 + 8p_1^{02})}, \\ \cos\alpha &= \cos\theta\cos\rho + \sin\theta\sin\rho\cos\varphi, \qquad \cos\rho = \frac{|\boldsymbol{q}|}{2|\boldsymbol{p}_1|}. \end{aligned}$$

Later to achieve the effective potential, one needs to make a Fourier transformation to Eq. (14)

$$V_{\mathrm{Im}_{\mathrm{box}(0^{-+})}}(r) = \int \mathrm{d}^3q V_{\mathrm{Im}_{\mathrm{box}(0^{-+})}}(\boldsymbol{q})\frac{\mathrm{e}^{\mathrm{i}\boldsymbol{q}\cdot\boldsymbol{r}}}{(2\pi)^3}, \quad (15)$$

and expand the expression with respect to $|\boldsymbol{p}_1|$. Because of the complexity of the integration, it is impossible to obtain an analytic expression, instead, we will calculate the corresponding part of the effective potential $V_{\mathrm{Im}_{\mathrm{box}}}$ and the matrix element $\langle\psi_0|V_{\mathrm{Im}_{\mathrm{box}}}|\psi_0\rangle$ numerically.

For the box diagram with ππ as the intermediate pseudoscalars (Fig. 2(b))

$$\begin{aligned}V_{\mathrm{Im}_{\mathrm{box}(0^{++})}}(\boldsymbol{q}) = 2g_{\mathrm{NN}\pi}^4\int\frac{\mathrm{d}^4l_1}{(2\pi)^4}\overline{v}(p_2)\gamma^5\frac{\not p_1-\not l_1+m_{\mathrm{p}}}{(p_1-l_1)^2-m_{\mathrm{p}}^2}\times\\ \gamma^5u(p_1)\overline{u}(p_3)\gamma^5\frac{\not p_3-\not l_1+m_{\mathrm{p}}}{(p_3-l_1)^2-m_{\mathrm{p}}^2}\gamma^5v(p_4)(\mathrm{i}\pi)^2\times\\ \delta(l_1^2-m_\pi^2)\delta\big[(p_1+p_2-l_1)^2-m_\pi^2\big]\times\\ \Big(\frac{\Lambda^2-m_{\mathrm{p}}^2}{(p_1-l_1)^2-\Lambda^2}\Big)^2\Big(\frac{\Lambda^2-m_{\mathrm{p}}^2}{(p_3-l_1)^2-\Lambda^2}\Big)^2, \quad (16)\end{aligned}$$

using the same method to deal with the above expression, we finally get

$$\begin{aligned}V_{\mathrm{Im}_{\mathrm{box}(0^{++})}}(r) = -\frac{1}{16\pi^2}\int\mathrm{d}^3q\frac{\mathrm{e}^{\mathrm{i}\,\boldsymbol{q}\cdot\boldsymbol{r}}}{(2\pi)^3}\int_0^{2\pi}\mathrm{d}\varphi\int_0^{\pi}\mathrm{d}\theta\sin\theta\times\\ \frac{2|\boldsymbol{l}_1^2|(\Lambda^2-m^2)^4}{24p_1^0\mathscr{B}(\mathscr{B}+2|\boldsymbol{l}_1||\boldsymbol{q}|\cos\alpha)(\mathscr{B}-\Lambda^2+m^2)^2}\times\\ \frac{1}{(\mathscr{B}-\Lambda^2+m^2+2|\boldsymbol{l}_1||\boldsymbol{q}|\cos\alpha)^2}, \quad (17)\end{aligned}$$

here

$$\begin{aligned}\mathscr{B} &= -2p_1^0l_1^0+2|\boldsymbol{p}_1||\boldsymbol{l}_1|\cos\theta+l_1^{0\,2}-\boldsymbol{l}_1^2,\\ l_1^0 &= \sqrt{m_\pi^2+\boldsymbol{l}_1^2},\\ |\boldsymbol{l}_1| &= \frac{1}{4p_1^0}\sqrt{16m_{\mathrm{p}}^4+2m_\pi^4-2m_\pi^2(m_\pi^2+8p_1^{0\,2})}.\end{aligned}$$

The imaginary part of the potential is a sum of the self-energy and the box contributions.

2.2.3 The width of the resonance

We take the imaginary part of the potential as a perturbation to evaluate the total width of the bound state. The legitimacy of this treatment will be discussed in the next section.

As we sandwich the imaginary part of the complex potential between $|\psi_0>$ which is the eigenstate of the Schrödinger equation with only real part of the effective potential and the expectation value is the imaginary part of the complex binding energy as

$$\mathrm{i}\,\Delta E_{\mathrm{imag}} = -\mathrm{i}\frac{\Gamma}{2} = \langle\psi_0|\mathrm{i}V_{\mathrm{Im}}(r)|\psi_0\rangle,$$

and

$$\mathrm{i}\,V_{\mathrm{Im}}(r)\equiv\mathrm{i}\,\Delta H_{\mathrm{imag}}.$$

Thus the total binding energy is

$$E = E_0+\Delta E_{\mathrm{real}}+\mathrm{i}\,\Delta E_{\mathrm{imag}} = E_0+\Delta E_{\mathrm{real}}-\mathrm{i}\frac{\Gamma}{2}.$$

It is noted that the contribution from the self-energy diagram to the imaginary potential is proportional to $\delta(\boldsymbol{r})$ function, thus

$$\langle\psi_0|\mathrm{i}\,V_{\mathrm{Im}}(r)|\psi_0\rangle\propto|\psi(0)|^2,$$

namely proportional to the wavefunction at origin. For the P-wave, $\psi(0)=0$, thus the self-energy diagram does not contribute to width of the P-wave.

The box diagram does contribute to both S-wave and P-wave states. To the P-wave, the contribution comes from the term which is proportional to $\boldsymbol{p}^2$. By the Weyl ordering[21], it should be written into a Hermitian form as

$$\begin{aligned}\frac{1}{4}[\boldsymbol{p}^2\mathscr{O}(m,m_\pi,\Lambda,r)+2\boldsymbol{p}\cdot\mathscr{O}(m,m_\pi,\Lambda,r)\boldsymbol{p}+\\ \mathscr{O}(m,m_\pi,\Lambda,r)\boldsymbol{p}^2],\end{aligned}$$

where $\mathscr{O}(m,m_\pi,\Lambda,r)\boldsymbol{p}^2$ is an operator in the configuration space. Thus,

$$\langle\psi|\boldsymbol{p}\cdot\mathscr{O}(m,m_\pi,\Lambda,r)\boldsymbol{p}|\psi\rangle\propto|\psi'(0)|^2,$$

is not zero for the P-wave.

3 Numerical results

By solving the Schrödinger equation, we obtain the zero-th order engenenergy and wavefunction, where the L-S coupling and tensor terms are taken as perturbations and the imaginary part of the complex potential is also treated as a perturbation. Following the traditional method of Quantum Mechanics, we can calculate the corrections to the mass spectrum corresponding to the real part of the energy and the total width of the bound state corresponding to the imaginary part of the energy.

We obtained the form factors and concerned parameters for the t-channel exchanges by fitting the deuteron spectrum, but the deuteron with constituents of proton and neutron does not possess an

s-channel annihilation. Therefore we may need an extra form factor which should reflect the annihilation suppression as discussed above. We adopt the form for the s-channel annihilation form factor as given in Eq. (10). If the bound state is in S-wave (0^{-+}), we take two schemes to determine the parameter α for calculating the total width below. One is that we use the upper bound on the width[1] 30MeV as input to detrmine the parameter α in the form factor (10), in another scheme, we take a typical value for the parameter $\alpha = 2m_{\rm p}$ and then recalculate the binding energy and width of the bound state. The numerical results are shown in Table 1 and Table 2.

Table 1. The binding energy and width with different σ-masses, where we set $\Gamma_{\rm s} = 30{\rm MeV}/c^2$.

m_σ/GeV	Λ/GeV	$E_{\rm s}$/MeV	α/GeV
0.47	0.59	−19.31	2.33
0.48	0.60	−18.19	2.14
0.49	0.61	−17.16	2.04
0.50	0.62	−16.24	1.97
0.51	0.63	−15.40	1.93
0.52	0.64	−14.65	1.89
0.53	0.65	−13.98	1.85
0.54	0.66	−13.39	1.84
0.55	0.67	−12.86	1.83

Table 2. Setting $\alpha^2 = 4m_{\rm p}^2$, the binding energy and width with different σ-mass.

m_σ/GeV	Λ/GeV	$E_{\rm s}$/MeV	$\Gamma_{\rm s}$/MeV
0.47	0.59	−19.31	43.83
0.48	0.60	−18.19	40.54
0.49	0.61	−17.16	37.63
0.50	0.62	−16.24	35.06
0.51	0.63	−15.40	32.82
0.52	0.64	−14.65	30.87
0.53	0.65	−13.98	29.19
0.54	0.66	−13.39	27.76
0.55	0.67	−12.86	26.57

As indicated above, if p and $\bar{\rm p}$ are in a P-wave state, the s-channel annihilation does not contribute to the potential (both real and imaginary parts), thus the form factor which reflects the annihilation suppression does not show up. Only the box-diagram determines its width. With the same procedure as for the S-wave state, we obtain the numerical results for the P-wave bound state.

Table 3. The values for P-wave bound state.

m_σ/GeV	$\Lambda/(\times 10^{-1}{\rm GeV})$	$E_{\rm p}$/MeV	$\Gamma_{\rm p}$/MeV
0.47	8.26	0.40	8.19
0.48	8.51	0.48	8.61
0.49	8.76	0.61	8.99
0.50	9.02	0.63	9.41
0.51	9.28	0.72	9.78
0.52	9.54	0.80	10.12
0.53	9.81	0.87	10.45
0.54	10.08	0.94	10.90
0.55	10.35	1.08	10.98

For the theoretical calculations, we have employed the following parameters as inputs: $m = 0.938{\rm GeV}$; $m_\pi = 0.138{\rm GeV}$; $m_\rho = 0.77{\rm GeV}$; $m_\omega = 0.783{\rm GeV}$; $m_\eta = 0.547{\rm GeV}$; $m_{\eta'} = 0.958{\rm GeV}$; $m_{\rm f_0} = 0.98{\rm GeV}$; $m_{\rm a_0} = 0.98{\rm GeV}$[19] $g_{\rm NN\pi} = g_{\rm NN\sigma} = 13.5$; $g_{\rm NN\rho} = g_{\rm NN\omega} = 3.25$[22]; $\frac{g^2_{\rm NN\eta}}{4\pi} = 0.4$; $\frac{g^2_{\rm NN\eta'}}{4\pi} = 0.6$[23]; $\gamma_{\eta\eta\sigma} = 4.11{\rm GeV}^{-1}$; $\gamma_{\eta\eta'\sigma} = 2.65{\rm GeV}^{-1}$; $\gamma_{\eta\eta{\rm f_0}} = 1.72{\rm GeV}^{-1}$; $\gamma_{\eta\eta'{\rm f_0}} = -9.01{\rm GeV}^{-1}$; $\gamma_{\pi\eta{\rm a_0}} = -6.80{\rm GeV}^{-1}$; $\gamma_{\pi\eta'{\rm a_0}} = -7.80{\rm GeV}^{-1}$[24]; $g_{\eta\rho\rho} = -16{\rm GeV}^{-1}$[17, 25]. Here, we assume the coupling constants for η(1295) and η(1440) to be the same as the values of those coupling constants for η and η′.

The effective potential (real part only) for S-wave and P-wave states are shown in Fig. 3.

4 Conclusion and discussion

In this work, in terms of the linear σ model we investigate the spectrum and total width of the possible p$\bar{\rm p}$ bound states. We consider two possibilities that the observed enhancement is due to a p$\bar{\rm p}$ bound state in S- or P-wave, namely it is a 0^{-+} or 0^{++} resonance.

All the parameters employed in the calculations were obtained by fitting the data of deuteron, except an extra parameter corresponding to the s-channel annihilation. With the very precise measurement on the binding energy of deuteron and more or less accurate estimate of the s-d mixing and charge radius, there is only a narrow window in the parameter space[8];1) . Namely there is almost not much free room to adjust them, and the fact provides us with a

1)It is noted that for deuteron, proton and neutron do not annihilate, the s-channel form factor does not apply there, so that we need to determine this new parameter α for the p$\bar{\rm p}$ bound state.

solid basis for the theoretical calculations, as long as the model is employed. Therefore the newly observed resonance, if it is experimentally confirmed, we will have an opportunity to further testify the linear σ model. Moreover, since p and $\bar{\text{p}}$ can annihilate into a meson, the study on the total width which concerns the coupling of p and $\bar{\text{p}}$ with this meson can provide us some information about this meson. Due to the pole structure of the propagator, only the meson(s) with a mass which is closer to the mass of the bound state (1859MeV) makes substantial contribution, thus only η(1295) and η(1440) comply with all requirements of spin, isospin, parity and charge conjugation, etc. Especially, for a long while people suspect if η(1440) is a glueball or a mixture of glueball and quarkonium, the value we obtained here may help to identify this resonance.

We derive the effective potential between p and $\bar{\text{p}}$, we simply substitute it into the schrödinger equation to obtain the binding energy. We have also calculated the absorptive part of the concerned loops by the Cutkosky cutting rule and it becomes the imaginary part of the potential. Different from the deuteron case which is a bound state of pn, for the p$\bar{\text{p}}$ case, there exist s-channel processes (see the figures in the text), which can contribute a real part (the tree level meson exchange) to the potential and an imaginary part through the loop diagrams. In this work, we ignore the dispersive part of the loops because it depends on the renormalization scheme and only makes a correction to the leading contribution of the real part of the potential, but keep the absorptive part which is the only source of the imaginary part of the potential.

Indeed, we may solve the Schrödinger equation with a complex potential, but in this work, for simplicity and making sense, we only use the perturbation method to deal with the imaginary part of the potential. We will solve the equation with a complex potential in our next work.

It is also noted that due to the G-parity structure of the NN and N$\bar{\text{N}}$ systems where N refers to nucleons, the potentials contributed by σ and ρ are of the same sign for the NN and N$\bar{\text{N}}$ systems, but the potential induced by π^0 and ω should have opposite signs for the two systems[13, 14]. In fact, for the deuteron case, which is in the pn structure, the contribution of π^0 is repulsive, and so is that from ρ and ω. But for the p$\bar{\text{p}}$ system, π^0 and ω induce attractive potentials while the contribution induced by σ and ρ remains unchanged. It can qualitatively explain why the binding energy for p$\bar{\text{p}}$ (about -18MeV) is more negative than that for deuteron (about -2.22MeV). Indeed the G-parity conservation does not really hold, this argument may help us to gain some hints to analyze the results, even though concrete derivations do not invoke the principle. Even though the G-parity argument is not very trustworthy, the symmetry analysis based on the G-parity may offer a reasonable explanation to the obtained results to make sense.

For the P-wave case, where the wave function of origin is zero, i.e. $\psi(0) = 0$, one does not need to calculate the s-channel annihilation process. However, on the other side, the box diagram which also contributes an absorptive part can result in an imaginary potential and then determine the width of the P-wave bound state. In fact, since the fitted mass of the bound state is above $2m_{\text{p}}$, the angular momentum barrier prevents dissociation of the bound state. Thus besides the mechanism discussed above, i.e. the bound state would decay into η(η′)σ (S-wave) or ππ (P-wave) at the leading order, there exists a possibility that dissolution of the bound state can occur via the quantum tunnelling into free p and $\bar{\text{p}}$. This tunnelling rate can be evaluated by the WKB method and our numerical results show that it is much smaller than that of decays into two pseudoscalars via the box diagram.

Fig. 3 shows the effective potential for S-wave and P-wave respectively. The repulsive part at the region of small r is due to the vector-meson exchange. One also notes that for the S-wave, besides the repulsive core for small r the potential is attractive, whereas for the P-wave, there exists an angular barrier which results in an positive binding energy, i.e. the total mass of the P-wave resonance is above the threshold of $2m_{\text{p}}$.

In our calculations, even though the t-channel parameters and form factors are determined by fitting

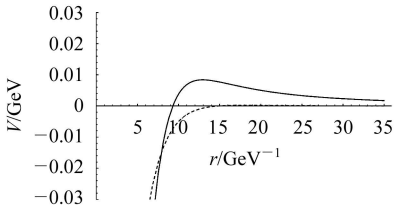

Fig. 3.

the accurately measured deuteron data, there is an extra form factor for the s-channel annihilation process and it reflects the annihilation suppression. Indeed, there is arbitrariness for adopting the form, but since we determine the parameter by fitting data, so that the model dependence would be partly removed or at least reduced to a trustworthy level. Moreover, when we evaluate the contribution of the annihilation, we only keep the lowest order and the self-energy of the mesons whose masses are closer to 1859MeV, such as $\eta(1295)$ and $\eta(1440)$, for the box-diagrams, we neglect the contributions from the vector mesons. All these approximations can bring certain theoretical errors. On the other side, as long as the measurement is not accurate, the experimental errors match the theoretical uncertaities. We can believe that the obtained results should be qualitatively correct, or can make sense. Once the resonance is more precisely measured, further theoretical work is obviously needed.

The newly observed enhancement by BES and Belle may have various interpretations, one of them is due to a resonance of $p\bar{p}$. In this work we discuss this possibility in the linear σ model and the obtained values are quantitatively consistent with the data. Our numerical results show that the total width and position of the proposed bound state, no matter it is in the S-wave or P-wave, do not contradict to the data. Therefore, either S-wave or P-wave state may be a possible state which can accommodate the observed enhancement.

The authors of[4] suggested an alternative explanation, i.e. the final state interaction results in the observed enhancement. To decide which mechanism is right or dominant would wait for the future experiments. We hope that studies on the new resonance can enrich our knowledge about the hadron physics and the interactions at the hadron level, especially get more information about the linear σ model. Our conclusion is that to confirm the observed enhancement, more precise measurements are needed.

We thank K.T. Chao for his helpful comments and suggestions, we also benefit from the fruitful discussions with C.H. Chang. We would especially thank B.S. Zou whose suggestions lead to some radical changes of the whole work. We are also indebted to S. Jin, X. Shen and other members of the BES Collaboration.

References

1 BAI J Z et al. Phys. Rev. Lett., 2003, **91**: 022001
2 Abe K et al. Phys. Rev. Lett., 2002, **88**: 181803
3 Abe K et al. Phys. Rev. Lett., 2002, **89**: 151802
4 ZOU B S, CHIANG H C. Phys. Rev., 2004, **D69**: 034004; Kerbikov B, Stavinsky A, Fedotov V. Phys. Rev., 2004, **C69**: 055205
5 Georgi H. Weak Interactions and Modern Particle Theory. New York: The Benjamin/Cummings Pub.Co., 1984
6 Machleidt R et al. Phys. Rep., 1987, **149**: 1
7 DAI Y B, WU Y L. Eur. Phys. J., 2005, **C39**: S1—S8
8 DING Y B et al. J. Phys., 2004, **G30**: 841—851
9 Bryan R, Phillips R. Nucl. Phys., 1968, **B5**: 201
10 Gourdin M, Jancovici B, Verlet L. IL NUOVO CIMENTO, 1958, **VIII**(3): 1413
11 Benresteskii V, Lifshitz E, Pitaeevskii L. Quantum Electrodynamics. New York: Pergamon Press, 1982
12 Gasiorowicz S. Quantum Mechanics. New York: Wiley Press, 1995
13 Klempt E et al. Phys. Rep., 2002, **368**: 119—316
14 Richard J M. Nucl. Phys. Proc., 2000, **86**(Suppl.): 361
15 Harada M. hep-ph/9606331; Sannino F, Schechter J. Phys. Rev., 1995, **D52**: 96—107; Black D et al. Phys. Rev., 1998, **D58**: 054012
16 Achasov N N, Kozhevnikov A A. Phys. Rev., 2000, **D62**: 056011
17 Lucio J et al. hep-ph/9902349; Gokalp A et al. Acta Phys. Polon., 2003, **B34**: 4095—4104; Wess J, Zumino B. Phys. Lett., 1971, **B37**: 65
18 Itzykson C, Zuber J B. Quantum Field Theory. New York: McGrow-Hill Press, 1980
19 The Data Group. Phys. Lett., 2004, **B592**: 1
20 Dover C, Richard J. Phys. Rev., 1980, **C21**: 1466
21 Lucha W, Schöberl F F, Gromes D. Phys. Rep., 1991, **200**(4): 127—240
22 LIN Z et al. Phys. Rev., 2000, **C61**: 024904; Holzenkamp B et al. Nucl. Phys., 1989, **A500**: 485; Janssen G et al. Phys. Rev. Lett., 1993, **71**: 1975

23 Tiator L, Bennhold C, Kamalov S S. Nucl. Phys., 1994, **A580**: 455—474
24 Black D et al. Phys. Rev., 2000, **D61**: 074030
25 Lublinsky M. Phys. Rev., 1997, **D55**: 249—254

Appendix A

In the Eq. (10), the leading part $V_0(r)$ is

$$\begin{aligned}V_0 = &\left(\frac{\mathrm{e}^{-\Lambda r}\Lambda g_{\mathrm{NN}\sigma}^2}{8\pi}-\frac{\mathrm{e}^{-\Lambda r}m_\sigma^2 g_{\mathrm{NN}\sigma}^2}{8\pi\Lambda}+\frac{\mathrm{e}^{-\Lambda r}g_{\mathrm{NN}\sigma}^2}{4\pi r}-\frac{\mathrm{e}^{-m_\sigma r}g_{\mathrm{NN}\sigma}^2}{4\pi r}\right)+\\ &\left(-\frac{\mathrm{e}^{-\Lambda r}\Lambda g_{\mathrm{NN}\rho}^2}{8\pi}+\frac{\mathrm{e}^{-\Lambda r}m_\rho^2 g_{\mathrm{NN}\rho}^2}{8\pi\Lambda}-\frac{\mathrm{e}^{-\Lambda r}g_{\mathrm{NN}\rho}^2}{4\pi r}+\frac{\mathrm{e}^{-m_\rho r}g_{\mathrm{NN}\rho}^2}{4\pi r}\right)+\\ &\left(\frac{\mathrm{e}^{-\Lambda r}\Lambda g_{\mathrm{NN}\omega}^2}{8\pi}-\frac{\mathrm{e}^{-\Lambda r}m_\omega^2 g_{\mathrm{NN}\omega}^2}{8\pi\Lambda}+\frac{\mathrm{e}^{-\Lambda r}g_{\mathrm{NN}\omega}^2}{4\pi r}-\frac{\mathrm{e}^{-m_\omega r}g_{\mathrm{NN}\omega}^2}{4\pi r}\right),\end{aligned}$$

the $\boldsymbol{L}\cdot\boldsymbol{S}$ coupling is

$$\begin{aligned}V_{(\boldsymbol{L}\cdot\boldsymbol{S})} = &\left[\left(\frac{\mathrm{e}^{-\Lambda r}g_{\mathrm{NN}\sigma}^2}{8m_{\mathrm{p}}^2\pi r^3}-\frac{\mathrm{e}^{-m_\sigma r}g_{\mathrm{NN}\sigma}^2}{8m_{\mathrm{p}}^2\pi r^3}+\frac{\mathrm{e}^{-\Lambda r}\Lambda g_{\mathrm{NN}\sigma}^2}{8m_{\mathrm{p}}^2\pi r^2}-\frac{\mathrm{e}^{-m_\sigma r}g_{\mathrm{NN}\sigma}^2 m_\sigma}{8m_{\mathrm{p}}^2\pi r^2}+\frac{\mathrm{e}^{-\Lambda r}\Lambda^2 g_{\mathrm{NN}\sigma}^2}{16m_{\mathrm{p}}^2\pi r}-\frac{\mathrm{e}^{-\Lambda r}m_\sigma^2 g_{\mathrm{NN}\sigma}^2}{16m_{\mathrm{p}}^2\pi r}\right)+\\ &\left(\frac{\mathrm{e}^{-\Lambda r}g_{\mathrm{NN}\rho}^2}{8m_{\mathrm{p}}^2\pi r^3}-\frac{\mathrm{e}^{-m_\rho r}g_{\mathrm{NN}\rho}^2}{8m_{\mathrm{p}}^2\pi r^3}+\frac{\mathrm{e}^{-\Lambda r}\Lambda g_{\mathrm{NN}\rho}^2}{8m_{\mathrm{p}}^2\pi r^2}-\frac{\mathrm{e}^{-m_\rho r}m_\rho g_{\mathrm{NN}\rho}^2}{8m_{\mathrm{p}}^2\pi r^2}+\frac{\mathrm{e}^{-\Lambda r}\Lambda^2 g_{\mathrm{NN}\rho}^2}{16m_{\mathrm{p}}^2\pi r}-\frac{\mathrm{e}^{-\Lambda r}m_\rho^2 g_{\mathrm{NN}\rho}^2}{16m_{\mathrm{p}}^2\pi r}\right)+\\ &\left(-\frac{\mathrm{e}^{-\Lambda r}g_{\mathrm{NN}\omega}^2}{8m_{\mathrm{p}}^2\pi r^3}+\frac{\mathrm{e}^{-m_\omega r}g_{\mathrm{NN}\omega}^2}{8m_{\mathrm{p}}^2\pi r^3}-\frac{\mathrm{e}^{-\Lambda r}\Lambda g_{\mathrm{NN}\omega}^2}{8m_{\mathrm{p}}^2\pi r^2}+\frac{\mathrm{e}^{-m_\omega r}m_\omega g_{\mathrm{NN}\omega}^2}{8m_{\mathrm{p}}^2\pi r^2}-\frac{\mathrm{e}^{-\Lambda r}\Lambda^2 g_{\mathrm{NN}\omega}^2}{16m_{\mathrm{p}}^2\pi r}+\frac{\mathrm{e}^{-\Lambda r}m_\omega^2 g_{\mathrm{NN}\omega}^2}{16m_{\mathrm{p}}^2\pi r}\right)\right](\boldsymbol{L}\cdot\boldsymbol{S}),\end{aligned}$$

the relativistic correction which in our later numerical computations is treated as a perturbation to the leading part, V_{pet} is

$$\begin{aligned}V_{\mathrm{pet}} = &\left(\frac{\mathrm{e}^{-\Lambda r}\Lambda^3 g_{\mathrm{NN}\sigma}^2}{8m_{\mathrm{p}}^2\pi}-\frac{\mathrm{e}^{-\Lambda r}\Lambda m_\sigma^2 g_{\mathrm{NN}\sigma}^2}{8m_{\mathrm{p}}^2\pi}+\frac{\mathrm{e}^{-\Lambda r}g_{\mathrm{NN}\sigma}^2}{4m_{\mathrm{p}}^2\pi r^3}-\frac{\mathrm{e}^{-m_\sigma r}g_{\mathrm{NN}\sigma}^2}{4m_{\mathrm{p}}^2\pi r^3}+\frac{\mathrm{e}^{-\Lambda r}\Lambda g_{\mathrm{NN}\sigma}^2}{4m_{\mathrm{p}}^2\pi r^2}-\right.\\ &\left.\frac{\mathrm{e}^{-m_\sigma r}m_\sigma g_{\mathrm{NN}\sigma}^2}{4m_{\mathrm{p}}^2\pi r^2}+\frac{\mathrm{e}^{-\Lambda r}\Lambda^2 g_{\mathrm{NN}\sigma}^2}{8m_{\mathrm{p}}^2\pi r}+\frac{\mathrm{e}^{-\Lambda r}m_\sigma^2 g_{\mathrm{NN}\sigma}^2}{8m_{\mathrm{p}}^2\pi r}-\frac{\mathrm{e}^{-m_\sigma r}m_\sigma^2 g_{\mathrm{NN}\sigma}^2}{4m_{\mathrm{p}}^2\pi r}\right)+\\ &\left(\frac{3\mathrm{e}^{-\Lambda r}\Lambda^3 g_{\mathrm{NN}\rho}^2}{32m_{\mathrm{p}}^2\pi}-\frac{3\mathrm{e}^{-\Lambda r}\Lambda m_\rho^2 g_{\mathrm{NN}\rho}^2}{32m_{\mathrm{p}}^2\pi}+\frac{\mathrm{e}^{-\Lambda r}g_{\mathrm{NN}\rho}^2}{4m_{\mathrm{p}}^2\pi r^3}-\frac{\mathrm{e}^{-m_\rho r}g_{\mathrm{NN}\rho}^2}{4m_{\mathrm{p}}^2\pi r^3}+\frac{\mathrm{e}^{-\Lambda r}g_{\mathrm{NN}\rho}^2\Lambda}{4m_{\mathrm{p}}^2\pi r^2}-\right.\\ &\left.\frac{\mathrm{e}^{-m_\rho r}g_{\mathrm{NN}\rho}^2 m_\rho}{4m_{\mathrm{p}}^2\pi r^2}+\frac{\mathrm{e}^{-\Lambda r}\Lambda^2 g_{\mathrm{NN}\rho}^2}{8m_{\mathrm{p}}^2\pi r}+\frac{\mathrm{e}^{-\Lambda r}m_\rho^2 g_{\mathrm{NN}\rho}^2}{16m_{\mathrm{p}}^2\pi r}-\frac{3\mathrm{e}^{-m_\rho r}m_\rho^2 g_{\mathrm{NN}\rho}^2}{16m_{\mathrm{p}}^2\pi r}\right)+\\ &\left(-\frac{3\mathrm{e}^{-\Lambda r}\Lambda^3 g_{\mathrm{NN}\omega}^2}{32m_{\mathrm{p}}^2\pi}+\frac{3\mathrm{e}^{-\Lambda r}\Lambda m_\omega^2 g_{\mathrm{NN}\omega}^2}{32m_{\mathrm{p}}^2\pi}-\frac{\mathrm{e}^{-\Lambda r}g_{\mathrm{NN}\omega}^2}{4m_{\mathrm{p}}^2\pi r^3}+\frac{\mathrm{e}^{-m_\omega r}g_{\mathrm{NN}\omega}^2}{4m_{\mathrm{p}}^2\pi r^3}-\frac{\mathrm{e}^{-\Lambda r}g_{\mathrm{NN}\omega}^2\Lambda}{4m_{\mathrm{p}}^2\pi r^2}+\right.\\ &\left.\frac{\mathrm{e}^{-m_\omega r}g_{\mathrm{NN}\omega}^2 m_\omega}{4m_{\mathrm{p}}^2\pi r^2}-\frac{\mathrm{e}^{-\Lambda r}\Lambda^2 g_{\mathrm{NN}\omega}^2}{8m_{\mathrm{p}}^2\pi r}-\frac{\mathrm{e}^{-\Lambda r}m_\omega^2 g_{\mathrm{NN}\omega}^2}{16m_{\mathrm{p}}^2\pi r}+\frac{3\mathrm{e}^{-m_\omega r}m_\omega^2 g_{\mathrm{NN}\omega}^2}{16m_{\mathrm{p}}^2\pi r}\right),\end{aligned}$$

and finally the tensor potential is

$$\begin{aligned}V_{\mathrm{tensor}} = &\left(\frac{\mathrm{e}^{-\Lambda r}\Lambda^3 g_{\mathrm{NN}\pi}^2}{96m_{\mathrm{p}}^2\pi}-\frac{\mathrm{e}^{-\Lambda r}\Lambda m_\pi^2 g_{\mathrm{NN}\pi}^2}{96m_{\mathrm{p}}^2\pi}+\frac{\mathrm{e}^{-\Lambda r}g^2}{16m_{\mathrm{p}}^2\pi r^3}-\frac{\mathrm{e}^{-m_\pi r}g_{\mathrm{NN}\pi}^2}{16m_{\mathrm{p}}^2\pi r^3}+\frac{\mathrm{e}^{-\Lambda r}\Lambda g_{\mathrm{NN}\pi}^2}{16m_{\mathrm{p}}^2\pi r^2}r-\right.\\ &\left.\frac{\mathrm{e}^{-m_\pi r}m_\pi g_{\mathrm{NN}\pi}^2}{16m_{\mathrm{p}}^2\pi r^2}+\frac{\mathrm{e}^{-\Lambda r}\Lambda^2 g_{\mathrm{NN}\pi}^2}{32m_{\mathrm{p}}^2\pi r}-\frac{\mathrm{e}^{-\Lambda r}m_\pi^2 g_{\mathrm{NN}\pi}^2}{96m_{\mathrm{p}}^2\pi r}-\frac{\mathrm{e}^{-m_\pi r}m_\pi^2 g_{\mathrm{NN}\pi}^2}{48m_{\mathrm{p}}^2\pi r}\right)+\\ &\left(-\frac{\mathrm{e}^{-\Lambda r}\Lambda^3 g_{\mathrm{NN}\rho}^2}{96m_{\mathrm{p}}^2\pi}+\frac{\mathrm{e}^{-\Lambda r}\Lambda m_\rho^2 g_{\mathrm{NN}\rho}^2}{96m_{\mathrm{p}}^2\pi}-\frac{\mathrm{e}^{-\Lambda r}g_{\mathrm{NN}\rho}^2}{16m_{\mathrm{p}}^2\pi r^3}+\frac{\mathrm{e}^{-m_\rho r}g_{\mathrm{NN}\rho}^2}{16m_{\mathrm{p}}^2\pi r^3}-\frac{\mathrm{e}^{-\Lambda r}\Lambda g_{\mathrm{NN}\rho}^2}{16m_{\mathrm{p}}^2\pi r^2}+\right.\end{aligned}$$

$$\frac{\mathrm{e}^{-m_\rho r}m_\rho g^2_{\mathrm{NN}\rho}}{16m_\mathrm{p}^2\pi r^2}-\frac{\mathrm{e}^{-\Lambda r}\Lambda^2 g^2_{\mathrm{NN}\rho}}{32m_\mathrm{p}^2\pi r}+\frac{\mathrm{e}^{-\Lambda r}m^2_\rho g^2_{\mathrm{NN}\rho}}{96m_\mathrm{p}^2\pi r}+\frac{\mathrm{e}^{-m_\rho r}m^2_\rho g^2_{\mathrm{NN}\rho}}{48m_\mathrm{p}^2\pi r}\Bigg)+$$
$$\Bigg(\frac{\mathrm{e}^{-\Lambda r}\Lambda^3 g^2_{\mathrm{NN}\omega}}{96m_\mathrm{p}^2\pi}-\frac{\mathrm{e}^{-\Lambda r}\Lambda m^2_\omega g^2_{\mathrm{NN}\omega}}{96m_\mathrm{p}^2\pi}+\frac{\mathrm{e}^{-\Lambda r}g^2_{\mathrm{NN}\omega}}{16m_\mathrm{p}^2\pi r^3}-\frac{\mathrm{e}^{-m_\omega r}g^2_{\mathrm{NN}\omega}}{16m_\mathrm{p}^2\pi r^3}+$$
$$\frac{\mathrm{e}^{-\Lambda r}\Lambda g^2_{\mathrm{NN}\omega}}{16m_\mathrm{p}^2\pi r^2}-\frac{\mathrm{e}^{-m_\omega r}m_\omega g^2_{\mathrm{NN}\omega}}{16m_\mathrm{p}^2\pi r^2}+\frac{\mathrm{e}^{-\Lambda r}\Lambda^2 g^2_{\mathrm{NN}\omega}}{32m_\mathrm{p}^2\pi r}-\frac{\mathrm{e}^{-\Lambda r}m^2_\omega g^2_{\mathrm{NN}\omega}}{96m_\mathrm{p}^2\pi r}-$$
$$\frac{\mathrm{e}^{-m_\omega r}m^2_\omega g^2_{\mathrm{NN}\omega}}{48m_\mathrm{p}^2\pi r}\Bigg)\left[\frac{3(\boldsymbol{\sigma}_1\cdot\boldsymbol{r})(\boldsymbol{\sigma}_2\cdot\boldsymbol{r})}{r^2}-(\boldsymbol{\sigma}_1\cdot\boldsymbol{\sigma}_2)\right],$$

and an extra term

$$V_{(\boldsymbol{\sigma}_1\cdot\boldsymbol{\sigma}_2)}=\left(\frac{\mathrm{e}^{-\Lambda r}\Lambda^3 g^2_{\mathrm{NN}\pi}}{96m_\mathrm{p}^2\pi}-\frac{\mathrm{e}^{-\Lambda r}\Lambda m^2_\pi g^2_{\mathrm{NN}\pi}}{96m_\mathrm{p}^2\pi}+\frac{\mathrm{e}^{-\Lambda r}m^2_\pi g^2_{\mathrm{NN}\pi}}{48m_\mathrm{p}^2\pi r}-\frac{\mathrm{e}^{-m_\pi r}m^2_\pi g^2_{\mathrm{NN}\pi}}{48m_\mathrm{p}^2\pi r}\right)+$$
$$\left(\frac{\mathrm{e}^{-\Lambda r}\Lambda^3 g^2_{\mathrm{NN}\rho}}{48m_\mathrm{p}^2\pi}-\frac{\mathrm{e}^{-\Lambda r}\Lambda m^2_\rho g^2_{\mathrm{NN}\rho}}{48m_\mathrm{p}^2\pi}+\frac{\mathrm{e}^{-\Lambda r}m^2_\rho g^2_{\mathrm{NN}\rho}}{24m_\mathrm{p}^2\pi r}-\frac{\mathrm{e}^{-m_\rho r}m^2_\rho g^2_{\mathrm{NN}\rho}}{24m_\mathrm{p}^2\pi r}\right)+$$
$$\left(-\frac{\mathrm{e}^{-\Lambda r}\Lambda^3 g^2_{\mathrm{NN}\omega}}{48m_\mathrm{p}^2\pi}+\frac{\mathrm{e}^{-\Lambda r}\Lambda m^2_\omega g^2_{\mathrm{NN}\omega}}{48m_\mathrm{p}^2\pi}-\frac{\mathrm{e}^{-\Lambda r}m^2_\omega g^2_{\mathrm{NN}\omega}}{24m_\mathrm{p}^2\pi r}+\frac{\mathrm{e}^{-m_\omega r}m^2_\omega g^2_{\mathrm{NN}\omega}}{24m_\mathrm{p}^2\pi r}\right)(\boldsymbol{\sigma}_1\cdot\boldsymbol{\sigma}_2).$$

线性σ模型和在$\mathrm{J/\psi}\to\gamma\mathrm{p\bar{p}}$的$\mathrm{p\bar{p}}$质量谱中观测到的增强现象*

刘翔[1] 曾小强[1] 丁亦兵[3] 李学潜[1,2;1)] 申虹[1] 沈彭年[2,4]

1 (南开大学物理系 天津 300071)
2 (中国科学院理论物理研究所 北京 100080)
3 (中国科学院研究生院 北京 100049)
4 (中国科学院高能物理研究所 北京 100049)

摘要 假定BES合作组在辐射衰变$\mathrm{J/\psi}\to\gamma\mathrm{p\bar{p}}$中观测到的$\mathrm{p\bar{p}}$谱的增强是由于存在一个$\mathrm{p\bar{p}}$的分子态, 用线性σ模型计算了它的束缚能和寿命. 具体考虑了这种增强现象是由于$\mathrm{p\bar{p}}$可能形成一个S波或P波共振态, 并把计算结果和实验数据做了比较. 与氘核不同, 由于$\mathrm{p\bar{p}}$可以通过s道湮没, 因此通过研究它的总宽度可以获得线性σ模型及其相关问题的信息.

关键词 线性σ模型 $\mathrm{J/\psi}$衰变 共振态 湮没

2005 – 06 – 20 收稿, 2005 – 08 – 09 收修改稿

*国家自然科学基金(10475202, 10475089, 10435080), 高等学校博士学科点专项科研基金, 中国科学院知识创新工程重大方向性项目(KJCX2-SW-N02)和中国科学院高能物理研究所创新基金(U529)

1) E-mail: lixq@nankai.edu.cn